Lipidomics study in liver metabolic diseases

Singh, M.

Chapter 3

A comparison between different human hepatocyte models reveals profound differences in net glucose production, lipid composition and metabolism *in vitro*

Based on

A comparison between different human hepatocyte models reveals profound differences in net glucose production, lipid composition and metabolism *in vitro*

Flavio Bonanini*, **Madhulika Singh***, Hong Yang, Dorota Kurek, Amy C Harms, Adil Mardinoglu, Thomas Hankemeier

Experimental Cell Research, Volume 437, Issue 1, 1 April 2024, 114008.
https://doi.org/10.1016/j.yexcr.2024.114008

*authors contributed equally

Abstract

Hepatocytes are responsible for maintaining a stable blood glucose concentration during periods of nutrient scarcity. The breakdown of glycogen and *de novo* synthesis of glucose are crucial metabolic pathways deeply interlinked with lipid metabolism. Alterations in these pathways are often associated with metabolic diseases with serious clinical implications. Studying energy metabolism in human cells is challenging. Primary hepatocytes are still considered the golden standard for *in vitro* studies and have been instrumental in elucidating key aspects of energy metabolism found *in vivo*. As a result of several limitations posed by using primary cells, a multitude of alternative hepatocyte cellular models emerged as potential substitutes. Yet, there remains a lack of clarity regarding the precise applications for which these models accurately reflect the metabolic competence of primary hepatocytes. In this study, we compared primary hepatocytes, stem cell-derived hepatocytes, adult donor-derived liver organoids, immortalized upcyte-hepatocytes and the hepatoma cell lines HepG2 in their response to a glucose production challenge. We observed the highest net glucose production in primary hepatocytes, followed by organoids, stem-cell derived hepatocytes, upcyte-hepatocytes and HepG2 cells. Gluconeogenic gene induction was observed in all tested models, as indicated by an increase in *G6PC* and *PCK1* expression. Lipidomics revealed considerable differences across the models, with organoids showing the closest similarity to primary hepatocytes in the common lipidome, comprising 347 lipid species across 17 classes. Changes in lipid profiles as a result of the glucose production induction suggest that only primary hepatocytes and organoids activate the fatty acid beta-oxidation pathway, resulting in decreased triglyceride content.

Keywords

Hepatocytes; *in vitro* glucose production; Lipidomics; Organoids; Energy metabolism

1. Introduction

Maintaining a stable blood glucose concentration through periods of nutrient availability or fasting is an essential physiological equilibrium [1]. Much of this balance is orchestrated by hepatocytes in the liver, which control several metabolic pathways to regulate glucose blood levels, such as glycogenesis, glycogenolysis, glycolysis, and gluconeogenesis [2]. During periods when a dietary glucose supply is not available, hepatocytes can secrete large quantities of glucose into the blood. Glucose is produced and released either via breakdown of stored glycogen (glycogenolysis and glycophagy) [3,4] or *de novo* synthesis using carbon substrates such as pyruvate, lactate and amino acids (gluconeogenesis) [5].

Lipid metabolism plays a crucial role in maintaining energy homeostasis and is deeply interlinked with glucose metabolism [6]. Gluconeogenesis is an energy-demanding process, which is primarily derived from the beta-oxidation of fatty acids (FAs). These FAs are stored in hepatocytes as triglycerides (TGs) or delivered by the adipose tissue via the blood circulation during periods of starvation [7]. The breakdown of FAs produces molecules such as acetyl-CoA and NADH, which can enter the Krebs cycle and the electron transport chain, respectively, to generate ATP that is necessary for the production of glucose [7]. While the link between fatty acid beta-oxidation and gluconeogenesis is widely accepted and characterized, the metabolic connection with other lipids, such as phospholipids and sphingolipids is complex and partially unknown.

Unsurprisingly, impaired or dysregulated glucose production and lipid metabolism, often associated with pathologies such as diabetes, obesity and inborn errors of metabolism, can lead to severe and life-threatening medical conditions [8–15]. Studying the process of glucose and lipid metabolism during periods of nutrient deprivation is crucial to understand how metabolic disorders lead to potentially life-threatening scenarios. Consequently, *in vitro* glucose production assays, in which hepatocytes are stimulated to secrete glucose under controlled conditions are central biological readouts that hold immense importance in the field. These assays rely on metabolically competent human hepatocyte models, experimental conditions that simulate the physiological nutrient availability oscillations found *in vivo* and robust assay to quantify molecular targets.

Primary human hepatocytes (PHH) are still considered as the gold standard in metabolic disease research but present several limitations, such as their limited availability, donor-to-donor variation, rapid de-differentiation and high costs. Hence, researchers have been exploring the

possibility to use alternative hepatocyte sources. Studies have reported comparison of PHH with iPSC-derived hepatocytes (iPSC-Hep) and HepG2 [16]. Glucose production has been measured for PHH, iPSC-derived hepatocytes and hepatoma cell lines and typically involve a prolonged period of starvation (3-24 h) in which the cells are cultured in absence (or reduced levels) of glucose but in presence of gluconeogenic substrates, such as glycerol, lactate or pyruvate [16–20].

Recently, expandable primary hepatocytes (Upcyte-Hep) have been generated by inducing low expression of the human papilloma virus [21,22] but their competence for energy metabolism studies remains doubtful [23]. Furthermore, hepatic organoids (Orgs) emerged as an exciting possibility to generate patient-derived expandable hepatocytes and recent progress started to determine their exact application landscape to study liver metabolism and disease [24,25]. Yet, more research is needed in order to identify specific applications of alternatives to primary hepatocytes in metabolism studies. Direct comparisons are needed for specific assays in order to evaluate the biological response of non-primary hepatocytes exposed to a metabolic challenge.

With this study, we aimed to characterize and compare the metabolic capabilities of various *in vitro* models of human hepatocytes such as iPSC-Hep, HepG2, Upcyte-Hep and organoids with PHH. Specifically, we challenged the models with a glucose production assay by measuring secreted glucose levels and induction of gluconeogenesis-related genes. Finally, we used a highly sensitive targeted lipidomics method to study the lipid profile of these hepatocyte models to monitor the modulation of intracellular lipid composition as a result of the glucose production challenge. This study aimed to further characterize and evaluate alternatives to primary hepatocyte models for energy metabolism studies.

2. Materials and methods

2.1 Cell culture

HepG2

HepG2 cells (Passage 3) were kindly provided by University of Groningen (order number: ATCC-HB-8065, ATCC, Manasses, Virginia, USA) and plated at 50000 cell/well in a 24 well plate. Cells were grown for 5 days in DMEM (Gibco, 11965092) + 10% Fetal Bovine Serum (FBS, Gibco, 16140071) + 1% Penicillin / Streptomycin with a full medium change every 2-3 days.

iPSC-Hep

iPSC-derived Hepatocytes (iCell Hepatocytes 2.0, Fujifilm) were cultured for 5 days in DMEM F12 (Thermo, 11039-021) supplemented with B27 (Thermo, 17504-044), 100 nM Dexamethasone (Sigma, D4902) and Gentamicin (Thermo, 15750-060). Then, cells were gently dissociated with TrypLE™ Express Enzyme (Thermo, 12604021) and seeded at 100000 cells/well in a collagen-I coated 24 well plates. Cells were grown for 5 days with a full medium change every 2-3 days.

PHH

Primary human hepatocytes (BIOIVT, M00995, Lot: MLS) were seeded at 700000 cells/well in a collagen-I coated 24 well plate after thawing in INVITROGRO CP Medium (BIOIVT, Z99029). Cells were kept in culture for 5 days in INVITROGRO HI Medium (BIOIVT, Z99009) with a medium change every 2-3 days.

Upcyte-Hep

Human upcyte® Hepatocytes (BIOIVT, CHE002, Lot 151.03.20180822.1) were thawed in Thawing Medium (Upcyte technologies, MHE001) seeded at a density of 10000 cells/cm^2 in collagen-type I-coated T75 flasks (Thermo, 156499) and cultured in High-Performance Medium (HPM, Upcyte technologies, MHE003). Cells were then dissociated with TrypLE™ Express Enzyme (Thermo, 12604021) and cryopreserved. Cells were then subsequently thawed and plated at 100000 cells/well in a collagen-I coated 24 well plate and kept in culture for 5 days in High-Performance Medium (HPM, Upcyte technologies, MHE003) with a medium change every 2-3 days.

Organoids

Primary adult stem cell-derived liver organoids are expanding adult bile duct-derived bipotent progenitor cells that can be differentiated into functional hepatocytes. The organoid line (M17-00060) was obtained from the Hubrecht Organoid Technology and was isolated from a healthy 43-year old male. Prior differentiation, organoids were maintained in HepatiCult^{TM} Growth Medium (STEMCELL Technologies, 100-0385) in droplets of 70% Matrigel GFR (7.2 mg/mL, Corning, 356237) and 30% HepatiCult Organoid Growth Medium (OGM, STEMCELL Technologies, 100-0385) with 50 µg/mL Primocin® (Invitrogen, ANT-PM-2) in 24-well suspension plates (Greiner Bio-One, 662102) in a humidified incubator at 37 °C, 5% CO_2 with an additional 500 µL per well of HepatiCult OGM [26]. Medium was refreshed every 2-3 days. Organoids were passaged by mechanical dissociation every 7-10 days. For passaging, the

Matrigel GFR droplets were broken using media from two wells and transferred to a 15 mL tube with a P1000 tip pre-coated with DBSA consisting of Dulbecco's Modified Eagle medium +4.5 g/L D-Glucose, L-Glutamine (Thermo, 31966047) with additional 1:100 v/v of PEN/STREP (Thermo, 15140122) and 1:100 v/v of 10% BSA (A2153, Sigma-Aldrich) in DPBS (Thermo, 14190144). A maximum of 12 wells were pooled in one 15 mL tube followed by filling it up to 12 mL with ice-cold DBSA and pipetting up and down 10 times using a 10 mL plastic pipette. The organoids were centrifuged at 450 rcf for 5 min at 8 °C (Eppendorf® Centrifuge 5910 R) and the supernatant was aspirated. The pellets were resuspended in 1 mL of AdDF+++, prepared by adding 1:100 v/v of GlutaMAX™ Supplement (Thermo, 35050061), 1:100 v/v of PEN/STREP (Thermo, 15140122), and 1:100 1M HEPES (15630080, Thermo Fisher) to Advanced DMEM/F-12 (12634028, Thermo Fisher). Organoids were sheared mechanically by pipetting up and down 10-20 times depending on donor and drop density with a P10 pipette tip fitted on a P1000 tip. AdDF+++ was added up to 12 mL and the tube was centrifuged at 450 rcf for 5 min at 8 °C. The supernatant was aspirated, and the pellet placed on ice before it was resuspended in OGM followed by addition of Matrigel GFR in a 30%-70% v/v ratio respectively, with a total volume of 50 µL per well to be seeded. Organoids were seeded in 50 µL droplets by pipetting them in the center of 24-well suspension plates that were pre-warmed at least 24 h in the incubator. After 5 min at room temperature (RT) the 24-well plates were placed upside down in the incubator for 1 h to solidify the droplets. Organoids used for this study were at passage 7.

Prior differentiation, organoids were cultured for 7 days in HepatiCult™ Growth Medium which was then replaced for additional 7 days with HepatiCult™ Differentiation Medium (STEMCELL Technologies, 100-0383). Full medium change was performed every 2-3 days. The research described here has been performed according to applicable Dutch national ethics regulations. The use of liver organoid line was approved by the medical ethical committee of the UMC Utrecht, the Netherlands in compliance with guidelines from Ethical Committee and European Union legislation.

2.2 Glucose production assay

2D cell cultures

To initiate the glucose production assay, the cell culture medium was replaced by pre-starvation medium comprised of DMEM + 2 mg/mL D-glucose (Sigma, G7021), 1 mM Sodium Pyruvate (Thermo, 11360070), 100 nM Dexamethasone (Sigma, D4902) and 1% Penicillin-Streptomycin (Sigma, P4333). Cells were cultured in pre-starvation medium for 2 h. Cells were

then washed 3 times with 1 mL glucose-free DMEM (Thermo, A1443001) to remove any residual glucose. Cells were then cultured for 12 h in either Glucose Production (GP) medium comprised of glucose-free DMEM supplemented with 1 mM Sodium Pyruvate, 20 mM Sodium Lactate (Sigma, L7022), GlutaMAX (Thermo, A1286001), 100 nM Dexamethasone (Sigma, D4902), 10 µM Forskolin (Tocris, 66575-29-9v), and 1% Penicillin-Streptomycin or, Fed medium comprised of DMEM supplemented with 2 mg/mL glucose, 1 mM Sodium Pyruvate, GlutaMAX, ITS (Thermo, 41400045), 100 nM Dexamethasone and and 1% Penicillin-Streptomycin.

3D cell culture

Organoids were extracted from Matrigel domes by mechanical dissociation in combination with cold Advanced DMEM/F-12 (Thermo, 12634028). Organoids were then collected in a 15 mL tube and more cold Advanced DMEM/F-12 was added for a final volume of 15 mL. The organoids were then centrifuged for 5 min at 450 g and 8 ºC. Matrigel layer was aspirated without disrupting the organoid pellet. 15 mL cold Advanced DMEM/F-12 was added to the tube, centrifuged and aspirated for a total of 2 washes. Matrigel-free organoids were then resuspended in 15 mL pre-starvation medium and incubated at 37 ºC for 2 h. After that, organoids were centrifuged, and pre-starvation medium was removed and replaced with 15 mL glucose-free DMEM. Organoids were washed with 15 mL glucose-free DMEM for 3 times and were then distributed across multiple 1.5 mL tubes in 1 mL glucose-free DMEM. Tubes were centrifuged at 300 g for 5 min at 8 ºC. Organoids were then resuspended in 200 µL of Fed (comprised of DMEM supplemented with 2 mg/mL glucose, 1 mM Sodium Pyruvate, GlutaMAX, ITS, 100 nM Dexamethasone and and 1% Penicillin-Streptomycin) or GP medium (comprised of glucose-free DMEM supplemented with 1 mM Sodium Pyruvate, 20 mM Sodium Lactate , GlutaMAX, 100 nM Dexamethasone, 10 µM Forskolin and 1% Penicillin-Streptomycin) for 12 h.

Glucose Measurement

To measure extracellular glucose, 250 µL of conditioned medium was collected in a 96 well-plate. 31.25 µL of 0.6 N HCl was added to inactivate endogenous enzyme activity and degrade NAD(P)H. After 5 min, 31.25 µL of 121 mg/mL Trizma base (Sigma, T1503) was added to neutralize the solution. To the remaining cells, 0.6 N HCl was added to extract intracellular glucose and was neutralized after 20 min using 121 mg/mL Trizma Base. Glucose was then measured by using Glucose-Glo (Promega, J6021) following manufacturer's instructions.

2.3 Protein quantification

Cells cultured in either GP medium or Fed medium for 12 h were lysed using 200 µL RIPA buffer (Thermo, 89900) for 10 min at room temperature. Total protein was then quantified using DC™ Protein Assay (BIO-RAD, 5000112).

2.4 qPCR

Total RNA was isolated from hepatocytes using RNeasy Mini Kit (Qiagen) and reverse transcribed using M-MLV Reverse Transcriptase (Invitrogen, 28025013) at 37 °C for 50 min in a - LightCycler® 96 Instrument (Roche, 05815916001). qPCR was performed using SYBR Green according to manufacturer's protocol. The primers used for the analysis were following: *G6PC* forward 5'-GCTGCTCATTTTCCTCATCAA-3', reverse 5'-TTCTGTAACAGCAATGCCTGA-3'; *PCK1* forward 5'-GGTCAGTGAGAGCCAACCAG-3', reverse 5'-AGATGGAGGAAGAGGGCATT-3'; *FBP1* forward 5'-GAGGCGTACGCTAAGGACTTT-3', reverse 5'-GAGGCGTACGCTAAGGACTTT-3'; *ACTB* forward 5'-CTCTTCCAGCCTTCCTTCCT-3', reverse 5'-AGCACTGTGTTGGCGTACAG3'.

2.5 Lipidomics analysis

Sample preparation

Cells cultured in either GP medium or Fed medium for 12 h were washed once with 1 mL cold PBS. Then, 250 µL of cold MeOH:Water 8:2 (v/v) was added. Adherent cells were scraped from the wells using a pipet tip, organoids were resuspended and disrupted and 100 µL was transferred to a tube. Samples were immediately frozen at -80 ºC.

Liquid chromatography-mass spectrometry (LC-MS) reagents and materials

The LC-MS grade acetonitrile and methanol and HPLC grade chloroform were purchased from Biosolve (Biosolve Chimie SARL), Dieuze, France. The ammonium acetate was of LC-MS grade (LiChropur™) and was purchased from Sigma-Aldrich (St.Louis, MO, USA). The Milli-Q® reference water purification system (Merck KGaA, Darmstadt, Germany) was used for purifying the water. The internal standard for lipidomics study was a mixture of splash lipidomix mix (330707-1EA); lysophosphatidylserine, LPS (17:1); lysophosphatidylinositol, LPI (17:1); lysophosphatidylglycerol, LPG (17:1) purchased from Avanti polar lipids. This internal standard mix also contained deuterated hexosyl ceramides, Hex-Cer 18:1;O2/16:0-d9 *(part no.-5040398)*; deuterated lactosyl ceramides, Lac-Cer 18:1;O2/16:0-d9 *(part no.-5040399*); deuterated dihydroceramides, Cer 18:0;O2/16:0-d9 *(part no.-5040397)*; deuterated

ceramides, Cer 18:1;O2/16:0-d9 *(part no.-5040167)* purchased from AB Sciex. The splash lipidomics mix contains deuterated internal standards mixture of phosphatidylcholine (PC); phosphatidylethanolamine (PE); phosphatidylserine (PS); phosphatidylglycerol (PG); phosphatidylinositol (PI); lysophosphatidylcholine (LPC); lysophosphatidylethanolamine (LPE); cholesteryl esters (CE); diglycerides (DG); triglycerides (TG); sphingomyelin (SM). The internal standard mixture was prepared in acetonitrile:methanol (3:7, v/v).

Lipid extraction

The lipids were extracted using Matyash method [27] with slight modifications. The tubes containing cells have 100 µL of methanol:water (80:20, v/v) were used for lipid extraction. 34 µL of the internal standard mix was added to each tube followed by the addition of 115 µL of methanol and 650 µL methyl *tert*-butyl ether (MTBE) and vortexed for 5 min. This mixture was then incubated at room temperature on an orbital shaker for 1 h. After the addition of water (143 µL), making the final ratio of MTBE:MeOH:Water to 10:3:2.5, v/v/v, the mixture was again incubated at room temperature for 10 min and centrifuged at 15800 rcf for 10 min at 4 °C. 550 µL of organic (upper) layer was collected and dried in a vacuum concentrator. Samples were then reconstituted with 150 µL of acetonitrile:methanol (3:7), vortexed and centrifuged for 10 min. The supernatant was taken and injected in LC-MS for analysis.

Lipid profiling through LC-MS analysis

Hydrophilic interaction chromatography with electrospray ionization-tandem mass spectrometry (HILIC-MS/MS) experiments were performed on an Exion LC AD (Sciex, Concord, ON,Canada) according to our previously published study [28]. The LC was coupled to QTRAP 6500+ mass spectrometer with a Turbo V source (Sciex, Concord, ON,Canada). Separations was performed on Luna amino column (100 mm × 2 mm, 3 µm, Phenomenex). The organic phase (MP-A) contains 1mM ammonium acetate in choroform: acetonitrile (1:9) and aqueous phase (MP-B) contains 1mM ammonium acetate in acetonitrile: water (1:1). The injection volume was kept 5 µL for all the classes except for TG and PE where it was kept at 1 µL. The temperature of the column was 35 °C. The rinsing solvent for the injector needle was isopropanol:water:dichloromethane (94:5:1, v/v/v). The mass spectrometer was operated at ionspray voltage of 5500 V and -4500 V for positive and negative mode respectively. The curtain gas was 20 psi, collision gas was kept at medium. The source temperature was 400 °C, GS1 and GS2 were 30 and 35 psi respectively. The data acquisition was done in scheduled MRM (sMRM) mode. The details about the sMRM window, ion transitions, retention times,

collision energy and declustering potential can be found in previous publication [28] and is summarized in **Table S2, sheet 1**. The total scan time was set at 0.5 sec. One internal standard per class has been used for the quantitation of lipid species. **Table S1** shows the concentration of internal standards spiked in the samples. Based on these concentrations and response of internal standards, the concentration of endogenous lipid species was calculated.

2.6 Data/Statistical analysis

Statistical analysis of glucose production rates was performed using GraphPad Prism 6.01. Significant differences at $p<0.05$ were determined using One-Way Anova, Dunnett's multiple comparison test. 'n' represents different well replicates. Gene expression analysis was performed using LightCycler®96. For lipidomics data, Sciex OS (v2.1.6) was used for peak integration and all statistical analyses were performed in R (version 4.2.0), and the packages such as ggplots, ggpubr, ComplexHeatmap were used to plot the graphs. The statistical significance was calculated using Kruskal-Wallis test followed by Dunnett's test.

3. Results

3.1 Hepatocyte glucose production

To compare the net glucose production of the hepatocyte models, we pre-cultured PHH, iPSC-Hep, Upcyte-Hep, HepG2 and organoids between 5 and 10 days under normal growth conditions. Then, medium was replaced with serum-free DMEM supplemented with 2 mg/mL glucose for 2 h prior to glucose production challenge as serum starvation has been shown to stimulate the induction of gluconeogenic genes [29]. The cells were then incubated with glucose production (GP) medium consisting of glucose-free and serum-free DMEM medium containing 20 mM lactate, 1 mM pyruvate, glutamine, 100 nM Dexamethasone and 10 µM Forskolin for 12 h (**Figure 1A**). Glucose levels were then measured both extracellularly and intracellularly. While detectable levels of extracellular glucose were measured for all hepatocyte models, PHH showed greater net glucose production and secretion (**Figure 1B**) followed by organoids, iPSC-Hep, Upcyte-Hep and HepG2. Similarly, intracellular levels were highest in PHH, followed by

organoids and iPSC-Hep while glucose concentration was below the detectable limit for Upcyte-Hep and HepG2 (**Figure 1B**).

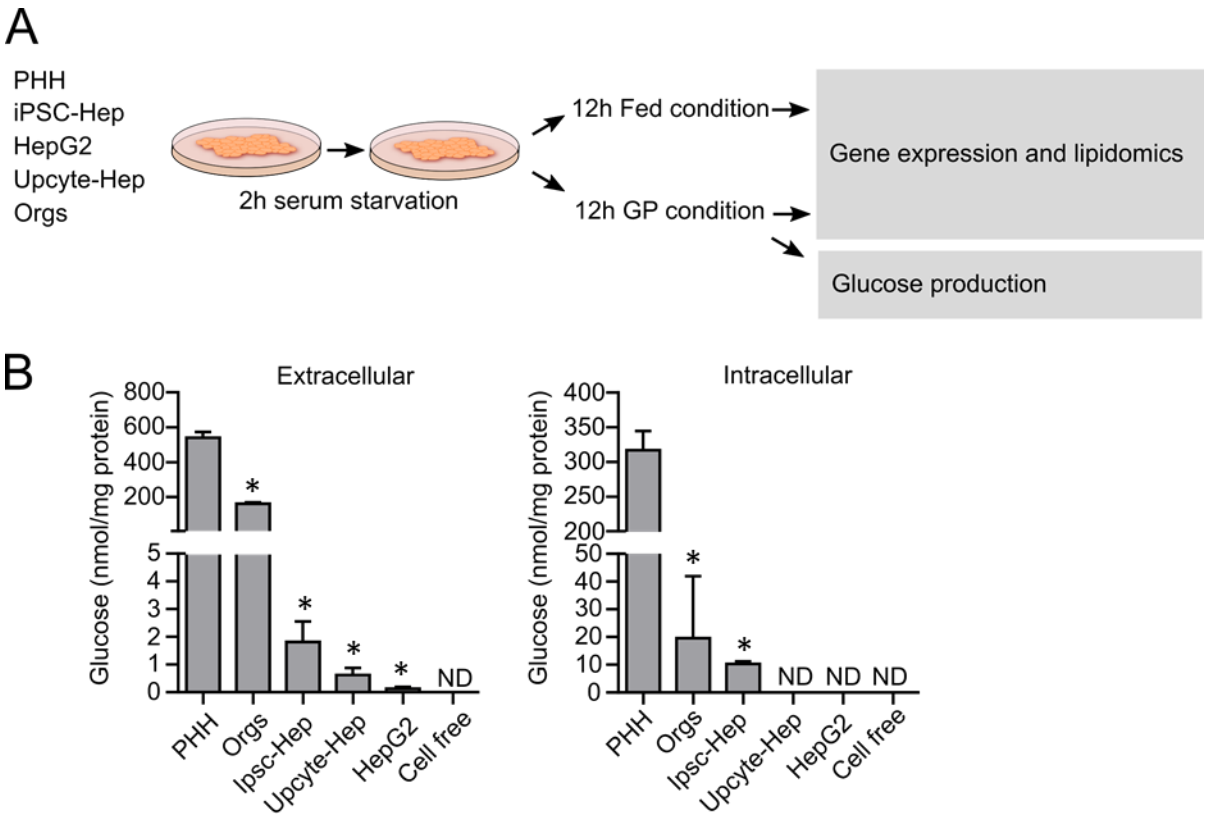

Figure 1. Experimental procedure and glucose production: (A) Scheme of the experimental procedure.; (B) Glucose production normalized to protein content after 12 h in GP medium. (n = 3-6; mean ± SD; *$p<0.05$, PHH Versus organoids (Orgs), iPSC-Hep, Upcyte-Hep, HepG2). n represents different well replicates.

3.2 Gluconeogenic genes induction

Gluconeogenesis is one of the main metabolic pathways for generation of glucose and becomes the dominant source of endogenously produced glucose after glycogen storages are depleted [7]. Gluconeogenesis is highly regulated on multiple levels including gene transcription [5]. Glucose-6-phosphatase (G6PC) hydrolyses the terminal step of gluconeogenesis and glycogenolysis. Phosphoenolpyruvate carboxykinase 1 (PCK1) is the rate-limiting enzyme of gluconeogenesis [30]. Fructose 1,6-biphosphatase (FBP1) converts fructose-1,6-biphosphate to fructose-6-phosphate in another rate-limiting reaction [5]. We assessed the gene expression levels of these key enzymes by qPCR for each hepatocyte model after 12 h of either GP medium or Fed medium. Overall, expression and induction of *G6PC* and *PCK1* were observed in all hepatocyte models (**Figure 2A**). *FBP1* appears to be the least regulated at a gene expression level and has notably low expresssion in HepG2 cells compared to the other gluconeogenic genes. PHH showed approximately 100-fold induction of *G6PC* and *PCK1* when cultured in

GP medium compared to Fed medium (**Figure 2B**). iPSC-Hep and Upcyte-Hep appear to regulate their gene expression levels in a comparable way to PHH while organoids showed overall reduced induction.

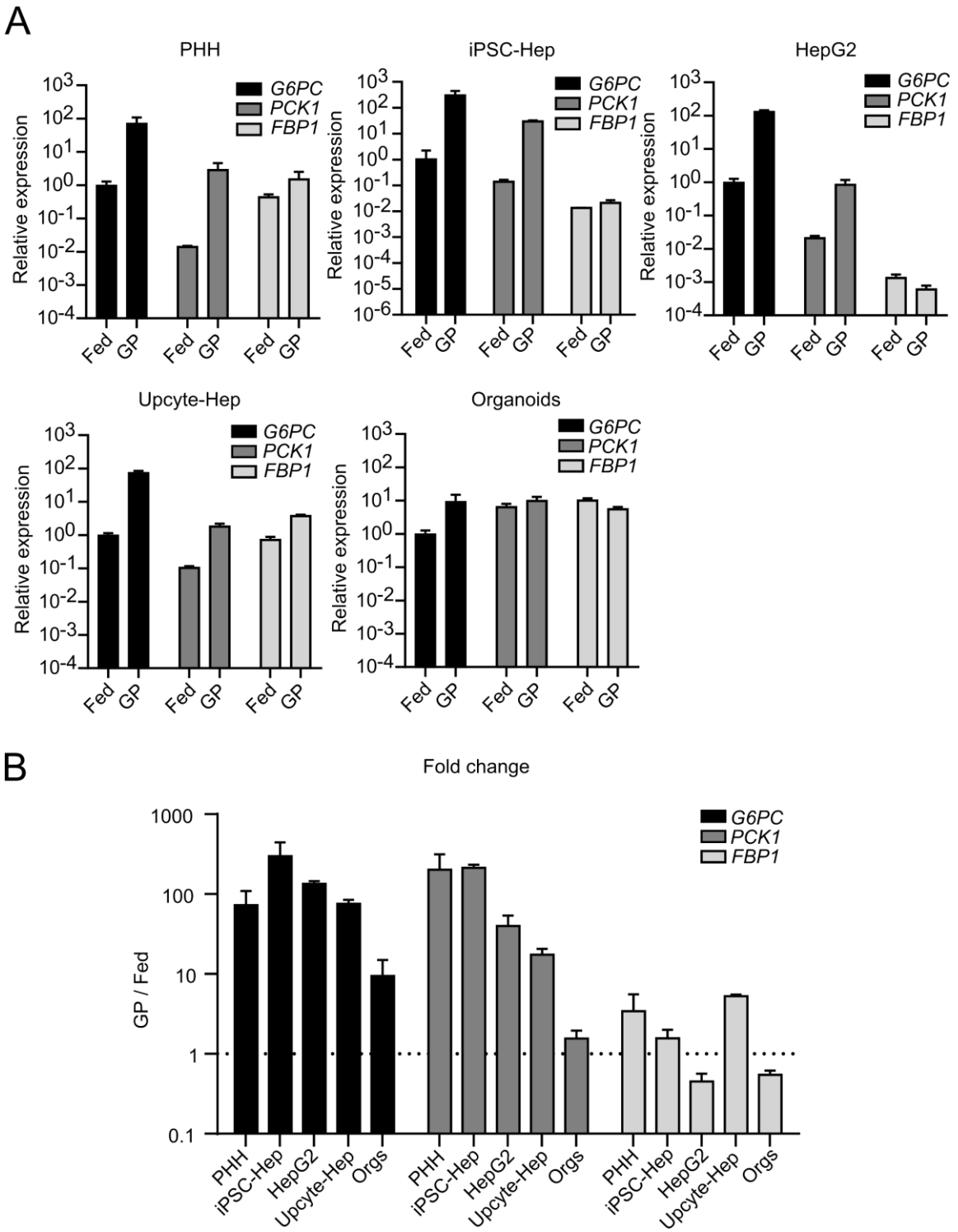

Figure 2. Gluconeogenesis gene induction as a result of glucose production challenge: (A) Expression of gluconeogenic genes in PHH, iPSC-Hep, HepG2 cells, Upcyte-Hep and organoids (Orgs) after 12 h incubation in GP or Fed medium. Genes of interest were normalized to the houskeeping gene ACTB and expression levels are

shown as relative to G6PC in Fed condition (n=3).; (B) Fold change of gene expression relative to the Fed condition for all hepatocyte models (n=3). n represents different well replicates.

3.3 Lipid profile of hepatocytes

Lipidomics analysis has been extensively used in metabolic studies of hepatocytes to profile entire cells or isolated lipid droplets [31–33]. We have used a HILIC-MS/MS method targeting 1200 lipid features for lipidomics analysis, where each feature represents one or more lipid species with certain chemical (sub)structures (i.e can include possible isomers). **Table 1** shows the total number of detected lipid species across 19 lipid (sub)classes in the hepatocyte models cultured with Fed or GP medium. These classes include phospholipids (LPE, PC, LPC, PI, PS, LPG, LPI, LPS, PG, PE, PE with alkyl ether (PE-O) and alkenyl ether substituents (PE-P)), sphingolipids (SM, HexCer, LacCer, Cer), glycerolipids (DG, TG) and sterol lipids (CE). We were able to detect 691 lipid species in PHHs, 624 in organoids, 433 in iPSC-Hep, 565 in Upcyte-Hep and 645 in HepG2 cells.

Table 1. The number of detected lipid species across 19 lipid (sub)classes in different hepatocyte models measured using HILIC-MS/MS.

Lipid class	HepG2	Upcyte-Hep	iPSC-Hep	PHH	Organoids	Common
LPE	16	18	11	24	24	8
PC	70	56	59	72	57	50
LPC	4	4	4	11	18	4
PI	35	26	21	59	48	20
PS	30	22	9	32	27	9
LPG	3	3	2	9	9	2
LPI	3	5	1	10	12	1
LPS	2	3	1	10	14	1
PG	47	43	39	55	42	33
SM	56	53	39	68	55	37
HexCer	9	10	3	18	14	3
LacCer	12	12	2	9	3	2
Cer	9	9	9	18	16	7
TG	253	207	174	169	171	123
PE	74	57	39	87	68	34
PE-O	14	18	8	20	22	6
PE-P	8	19	12	14	20	7
DG	0	0	0	4	2	0
CE	0	0	0	2	2	0
Total	***645***	***565***	***433***	***691***	***624***	***347***

First, we compared the total lipidome found in each hepatocyte model in Fed medium and divided the lipid species according to their chain length and amount of double bonds in

glycerolipids and phospholipids. **Figure 3A** shows abundance of lipid species containing chain lengths of 16, 18, 20 and 22 carbon atoms in glycerolipids and phospholipids (as these four were the most abundant fatty acid chains). In glycerolipids, PHH cells exhibit the greatest prevalence of FA chain lengths comprising 18 carbon atoms, followed by FA chain lengths containing 16 carbon atoms. For iPSC-Hep, the dominant FA chain length is 16 carbon atoms, followed by 18 carbon atoms. HepG2, Upcyte-Hep and organoids have comparable levels of abundance for 16 and 18 carbon containing FA chains. PHH cells also display lipid species with longer chain lengths like C20 and C22. Within phospholipids, species with 18 carbon chain length emerges as the most abundant across all cell types. The FA chain with 20 carbons is the second abundant chain in all the hepatocyte models except HepG2 where 16 carbons are the second abundant. C22 remains the least abundant chain length across all cell types, with PHH cells exhibiting the highest prevalence among the five hepatocyte models. **Figure 3B** illustrates the distribution of lipid species in glycerolipids and phospholipids based on the presence of monounsaturated fatty acids (MUFA), polyunsaturated fatty acids (PUFA), and saturated fatty acids (SFA) across the five cell models. Among glycerolipids, all hepatocyte models show higher prevalence of MUFA compared to primary hepatocytes and a lower content in PUFA. In phospholipids, PHH and iPSC-Hep cells shows the highest abundance in PUFA, while HepG2, Upcyte-Hep, and organoids have a higher presence of MUFA, followed by PUFA. Across all hepatocyte models, SFA shows a lower level of abundance in phospholipids. We also performed this analysis in the GP medium to investigate the variation in the composition of fatty acyl chains in lipids under glucose-deprived conditions. However, we observed a similar abundance of species in the GP medium as in the Fed medium.

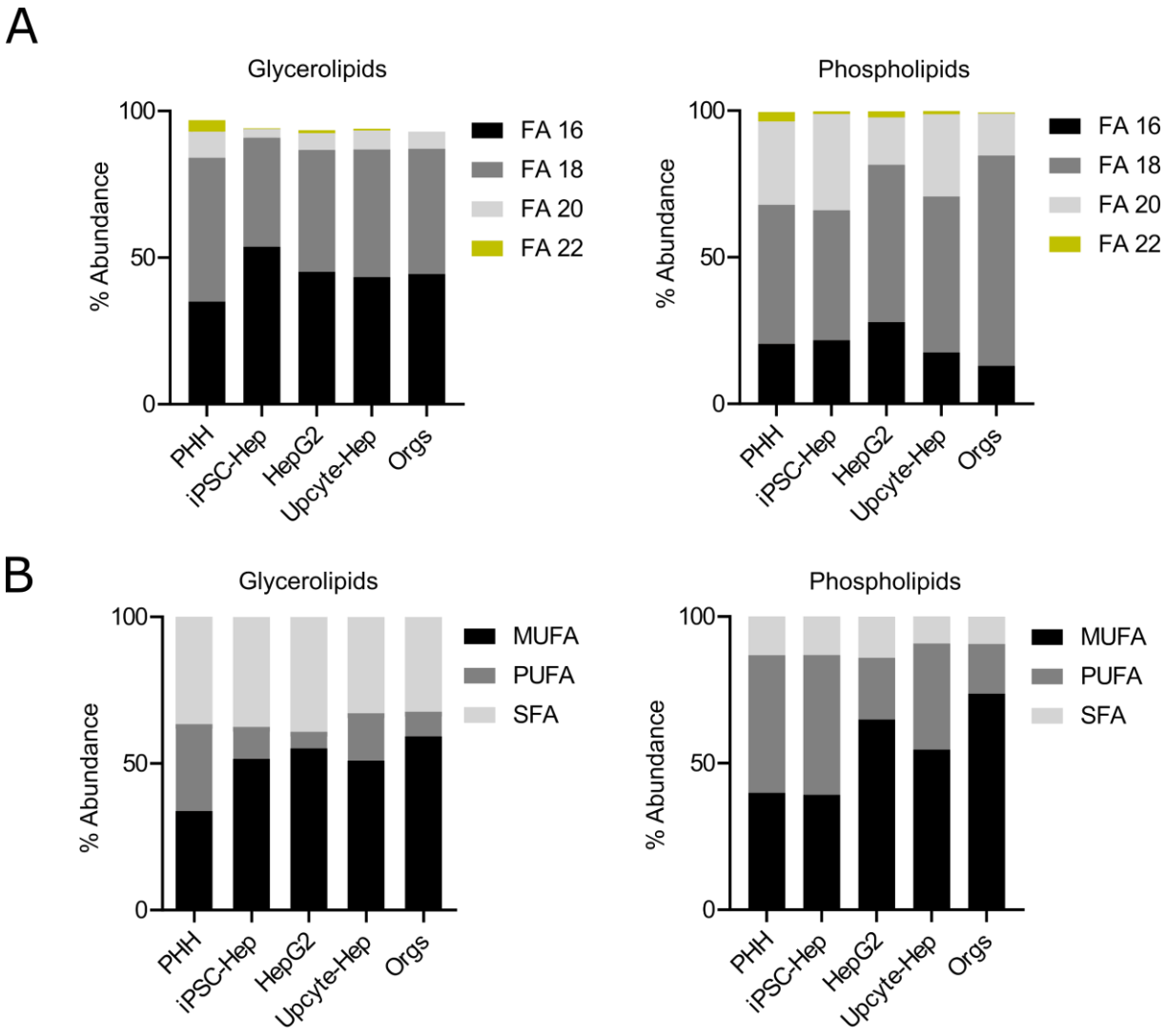

Figure 3. Fatty acyl chain composition of glycerolipids and phospholipids in five hepatocyte models in Fed medium. (A) Abundance (%) of lipids with fatty acid chain length containing 16, 18, 20 and 22 carbon atoms.; (B) Abundance (%) of lipids containing monounsaturated fatty acid (MUFA), polyunsaturated fatty acid (PUFA) and saturated fatty acid (SFA). In Figure 3A, the total does not add up to 100%, as there are also minor contributions from other chain lengths.

Since our aim was to identify similarities and differences of alternative hepatocyte models to PHH, we confined the consequent analysis only to the common species across the different models and samples reducing the number to 347 lipid species that were distributed across 17 lipid (sub)classes. The concentration of all the species in Fed and GP state are specified in **Table S2, sheet 2.** The accurate concentration of endogenous lipid species was calculated based on the concentration of internal standards spiked in the samples. The relative abundance of each class was calculated based on these concentrations. For this, we considered the amount of lipids in each distinct class divided by the total amount of lipids (as the sum of all species across all classes). In terms of relative abundance expressed in mol% across all common species, we found that in PHH the TG class constitutes the largest proportion of lipid species in both Fed

and GP conditions totaling approximately 60% followed by PC with about 22%, while PE, PI, SM and PS constitute approximately 6%, 5%, 4% and 2.5% of the common lipidome, respectively. Other lipid classes account for the remaining percentage. A similar ranking was observed for all hepatocyte models with the exception of Upcyte-Hep, where we found TGs to account for only 31%, with PC being the most abundant (34%). An extensive summary of the relative abundance is presented in **Table 2**.

Table 2. Composition of the lipidome of tested hepatocyte models under Fed and GP conditions expressed as mol% from the accurate amount of common lipid molecular species obtained by HILIC-MS/MS analysis.

mol%	Fed medium				
	PHH	**iPSC-Hep**	**HepG2**	**Upcyte-Hep**	**Organoids**
LPE	0.136 ± 0.003	0.145 ± 0.018	0.122 ± 0.005	0.256 ± 0.018	0.081 ± 0.007
PC	21.621 ± 1.038	15.421 ± 0.221	30.768 ± 0.758	33.6 ± 0.449	11.968 ± 0.501
LPC	0.141 ± 0.014	0.144 ± 0.011	0.086 ± 0.006	0.157 ± 0.015	0.102 ± 0.01
PI	4.725 ± 0.133	2.527 ± 0.03	4.833 ± 0.106	6.895 ± 0.584	2.656 ± 0.153
PS	2.455 ± 0.089	1.57 ± 0.048	5.39 ± 0.357	6.75 ± 0.313	1.578 ± 0.121
LPG	0.007 ± 0.001	0.007 ± 0.001	0.008 ± 0.001	0.03 ± 0.001	0.003 ± 0.001
LPI	0.041 ± 0.01	0.039 ± 0.004	0.023 ± 0.003	0.218 ± 0.035	0.018 ± 0.005
LPS	0.065 ± 0.012	0.034 ± 0.003	0.015 ± 0.002	0.123 ± 0.014	0.044 ± 0.01
PG	0.745 ± 0.051	0.6 ± 0.036	0.992 ± 0.043	2.189 ± 0.054	0.909 ± 0.039
SM	3.578 ± 0.056	2.279 ± 0.037	3.318 ± 0.042	5.579 ± 0.11	0.897 ± 0.052
HexCer	0.006 ± 0.001	0.013 ± 0.001	0.007 ± 0.001	0.034 ± 0.001	0.001 ± 0
LacCer	0.022 ± 0.003	0.003 ± 0	0.024 ± 0.001	0.039 ± 0.003	0.001 ± 0
Cer	0.67 ± 0.026	0.222 ± 0.012	0.112 ± 0.008	1.303 ± 0.17	0.26 ± 0.028
TG	59.664 ± 0.797	71.585 ± 0.883	45.623 ± 0.831	30.644 ± 0.577	77.948 ± 2.299
PE*	6.124 ± 0.176	5.411 ± 0.174	8.678 ± 0.198	12.184 ± 0.342	3.533 ± 0.17

mol%	Glucose production (GP) medium				
	PHH	**iPSC-Hep**	**HepG2**	**Upcyte-Hep**	**Organoids**
LPE	0.177 ± 0.004	0.145 ± 0.018	0.083 ± 0.001	0.282 ± 0.009	0.082 ± 0.008
PC	23.775 ± 0.374	15.421 ± 0.221	31.985 ± 0.929	34.478 ± 0.199	11.63 ± 0.503
LPC	0.202 ± 0.01	0.144 ± 0.011	0.105 ± 0.007	0.163 ± 0.008	0.113 ± 0.005
PI	4.993 ± 0.104	2.527 ± 0.03	4.723 ± 0.211	6.547 ± 0.347	2.874 ± 0.123
PS	2.547 ± 0.088	1.57 ± 0.048	6.872 ± 0.191	5.974 ± 0.108	1.414 ± 0.063
LPG	0.009 ± 0.001	0.007 ± 0.001	0.01 ± 0.001	0.039 ± 0	0.006 ± 0.001
LPI	0.042 ± 0.006	0.039 ± 0.004	0.031 ± 0.001	0.296 ± 0.041	0.017 ± 0.005
LPS	0.083 ± 0.015	0.034 ± 0.003	0.017 ± 0.001	0.124 ± 0.009	0.045 ± 0.015
PG	0.804 ± 0.032	0.6 ± 0.036	1.018 ± 0.019	2.064 ± 0.06	0.908 ± 0.099

SM	3.636 ± 0.057	2.279 ± 0.037	3.518 ± 0.075	5.672 ± 0.079	0.869 ± 0.045
HexCer	0.009 ± 0	0.013 ± 0.001	0.004 ± 0	0.025 ± 0	0.001 ± 0
LacCer	0.021 ± 0.001	0.003 ± 0	0.019 ± 0.002	0.033 ± 0.001	0.001 ± 0
Cer	0.688 ± 0.036	0.222 ± 0.012	0.12 ± 0.024	1.293 ± 0.034	0.253 ± 0.008
TG	58.298 ± 2.584	71.585 ± 0.883	45.166 ± 1.216	32.095 ± 0.572	78.607 ± 1.555
PE*	4.716 ± 0.068	5.411 ± 0.174	6.328 ± 0.264	10.917 ± 0.09	3.181 ± 0.149

***** The abundance of PE-O and PE-P were included in PE.

Principal component analysis (PCA) reveals a high degree of agreement between replicates but also distinct separation between the different models in both experimental conditions (**Figure 4**). This analysis suggests diverse lipid profiles for PHH and Organoids which appear to be constituting distinctly isolated, and iPSC-Hep, HepG2 and Upcyte-Hep which tend to cluster together in another separate group. Within this group, iPSC-Hep, HepG2 and Upcyte-Hep can further be distinguished from each other (**Figure 4**, insert) revealing closest similarity between iPSC-Hep and Upcyte-Hep, while HepG2 tends to cluster separately. Overall, we observed distinct separation between all hepatocyte models. In comparison to the difference across separate hepatocyte models, distinction between Fed and GP conditions within each model appear to be relatively limited. This suggests a small alteration of the lipidome as a result of the glucose production challenge in the condition studied.

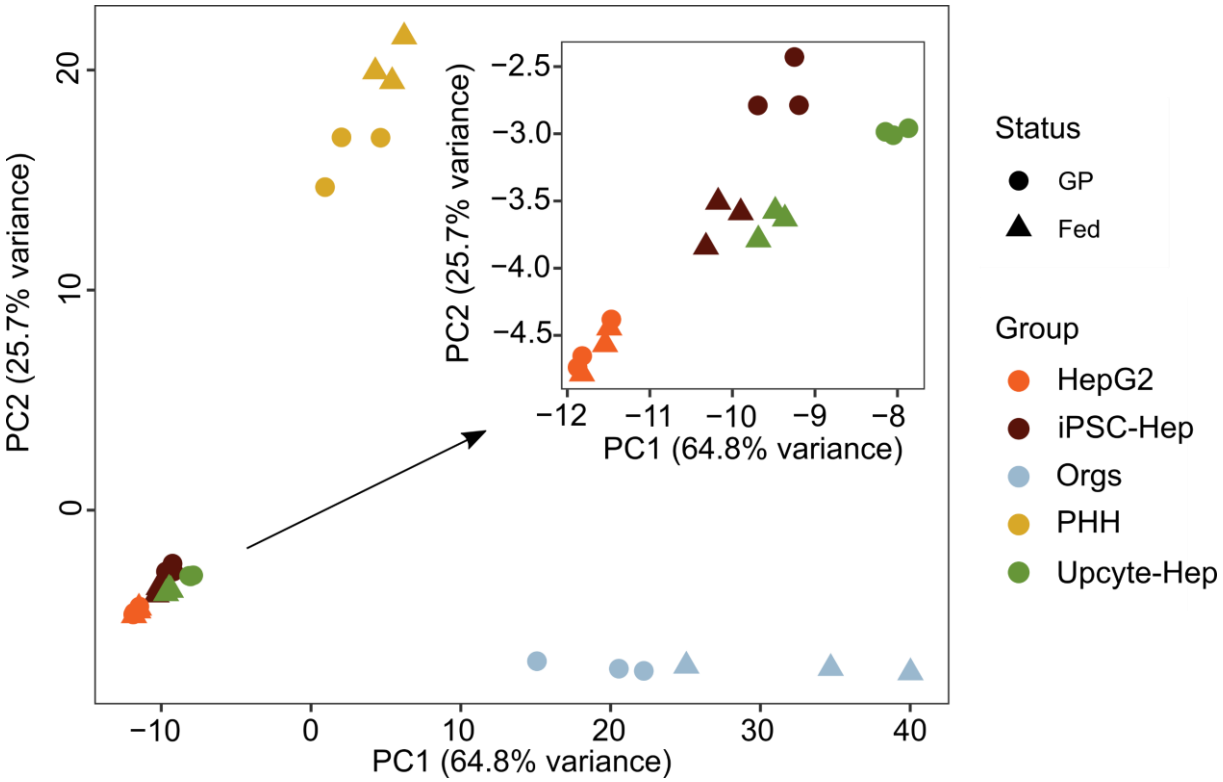

Figure 4. PCA plot showing the separation between hepatocyte models based on their lipid profile.

Further, we used a heatmap to visualize the abundance of lipid species. We confirmed the association between the hepatocytes by performing hierarchical clustering on the whole dataset (**Figure 5**). Overall, organoids show the highest lipid concentration across the lipidome, followed by PHH. The heatmap reveals closest similarity between the datasets of PHH and organoids, while confirming the separation of iPSC-Hep, HepG2 and Upcyte-Hep as a distinct group. **Table S2, sheet 3** presents the statistical significance of individual species, indicating the variation in their profiles across all four hepatocyte models when compared to PHH.

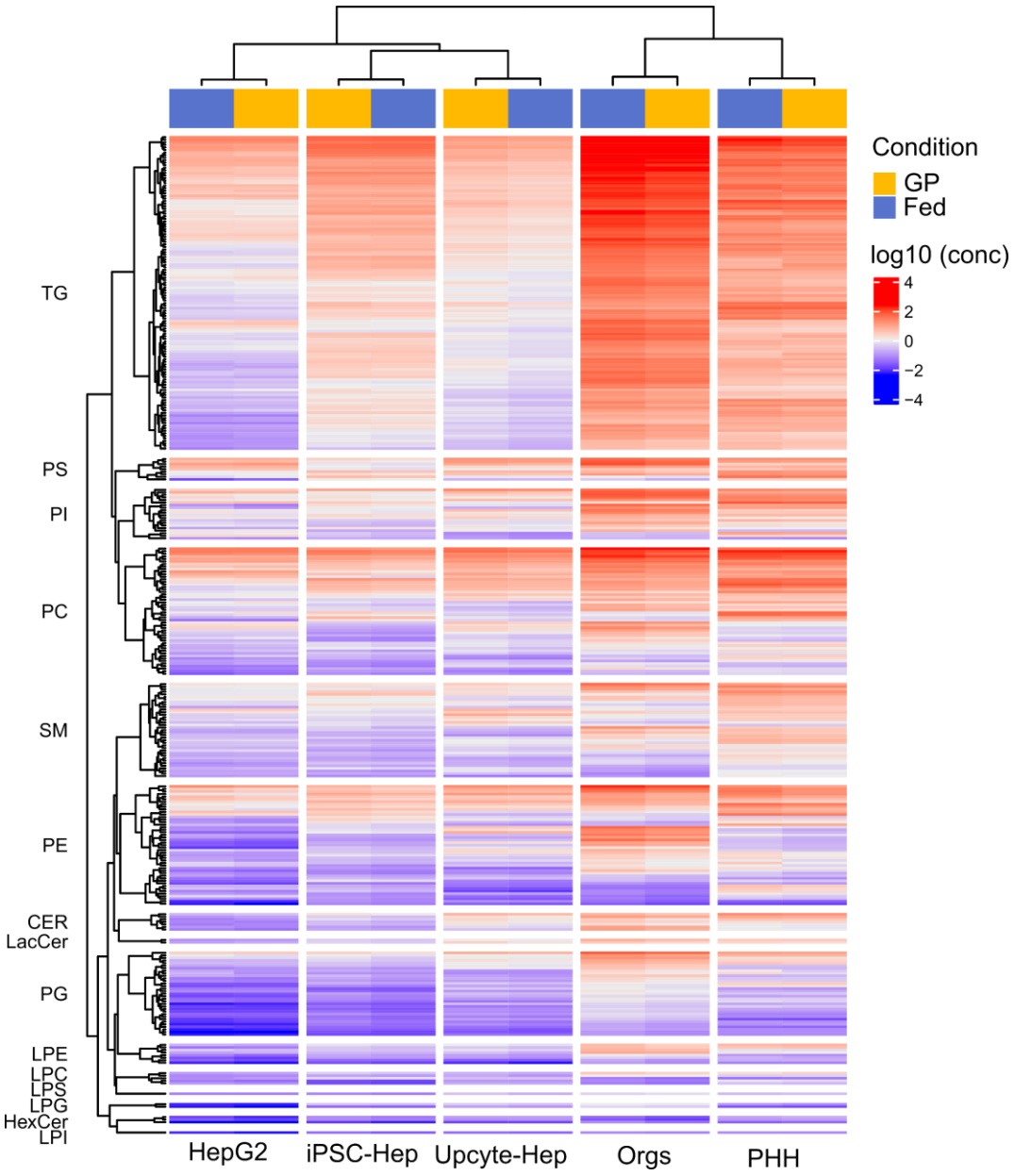

Figure 5. Heatmap of lipid species concentration, divided into their classes and associated dendograms. Each row represents a lipid species and color scale indicates log10 of the concentration normalized to protein content.

Experimental conditions, GP and Fed, did not cause drastic changes in the lipid profiles of the tested models. To evaluate significant changes in lipid species concentrations resulting from glucose production induction conditions, we conducted a statistical analysis (using $FC \geq 1.5$ *or* $FC \leq 0.7$ and $p<0.05$). **Table 3** shows the lipid species that have been altered during GP conditions. Here we observed significant downregulation of 18 TG species and 21 PE species in PHH while there were no significant changes in the other lipid classes. This was in strong contrast with the other hepatocyte models where we observed a diverse response to the culture conditions. iPSC-Hep show an increase in several classes while no change in TG was observed. HepG2 cells revealed only minimal significant changes with a possible exception of a few species in PE, LPE, PI and PC. Upcyte-Hep shows a marked increase in several classes, most notably PC and TG. In contrast, organoids showed a significant decrease across most of the species in the lipidome including 18 PC species, 28 TG species and 32 PE species. The identity of the species that have been altered in the GP medium has been provided in **Table S2, sheet 4.** We noted that GP medium caused a reduction of saturated species in organoids like PC 18:0_18:0, PE 16:0_16:0 and PC 16:0_16:0. Conversely, we observed an elevation in species containing PUFA such as PC 16:0_20:4, PC 18:1_20:4 and PG 18:2_20:4 in iPSC-Hep, HepG2 and Upcyte-Hep. This might indicate an overall preference for saving PUFAs in fasting conditions to preserve essential building blocks for membrane synthesis or provide substrate for enzymatic reactions to produce signaling molecules.

Table 3. Lipidome alterations during GP conditions listing the number of lipid species that have been either increased or decreased during the GP state.

Lipid classes	*Increased*					*Decreased*				
	PHH	iPSC-Hep	HepG2	Upcyte-Hep	Organoids	PHH	iPSC-Hep	HepG2	Upcyte-Hep	Organoids
LPE	0	0	0	1	0	0	0	4	0	3
PC	0	6	3	12	0	0	0	0	0	18
LPC	0	0	0	2	0	0	0	0	0	1
PI	0	1	0	3	0	0	0	4	0	1
PS	0	0	1	0	0	0	0	0	0	5
LPG	0	1	0	1	0	0	0	0	0	0
LPI	0	0	0	1	0	0	0	0	0	0
LPS	0	0	0	0	0	0	0	0	0	0
PG	0	13	0	1	0	0	0	2	0	7
SM	0	1	0	1	0	0	0	0	0	9
HexCer	0	2	0	0	0	0	0	2	0	3
LacCer	0	0	0	0	0	0	0	0	0	1
Cer	0	2	1	1	0	0	0	1	0	3
TG	0	0	2	31	0	18	0	1	0	28

PE; PE-O; PE-P	0	3	0	0	0	21	0	9	0	32

4. Discussion

This study reaffirmed the distinct responses that different hepatocyte models may produce under a metabolic challenge *in vitro*. We challenged primary hepatocytes, iPSC-derived hepatocytes, upcyte hepatocytes, hepatic organoids and HepG2 with a glucose production condition, in which the cells were starved of glucose for 12 h but stimulated with forskolin to induce expression of gluconeogenic genes and supplied with the gluconeogenic precursors pyruvate, lactate and amino acids. Forskolin directly stimulates the cyclic adenosine monophosphate (cAMP) signalling pathway which has been shown to mimic the action of glucagon on primary hepatocytes [34]. Glucose production assays rely on a net-positive balance between production and consumption, where glucose is measured in the conditioned medium after an incubation period.

Due to their metabolic competence and despite their limitations, primary hepatocytes have been routinely used in energy metabolism studies, including *in vitro* glucose production capacity and dose-dependent response to either insulin or glucagon [16]. In this study, we confirmed that primary hepatocytes are indeed capable of positive net glucose production and showed the highest value compared to all other tested models. Hepatoma cell line HepG2, a widely used hepatocyte model, showed the least net glucose production of the models tested. This is in line with evidence suggesting an aberrant phenotype in terms of glucose metabolism that doesn't represent liver energy metabolism [35]. Indeed, a study shows 14-fold greater glucose incorporation compared to primary hepatocytes after incubation with ^{14}C glucose suggesting a much higher consumption rate compared to primary hepatocytes. The same study also shows a decreased capacity of fatty acid oxidation [17].

iPSC-derived hepatocytes emerged as a promising alternative to primary hepatocytes as iPSCs are a virtually illimited source of cells, they carry the genetic profile of the donor and can differentiate into hepatocyte-like cells. iPSC has been proposed as a valid alternative and several studies show similar metabolic competence as primary hepatocytes including glucose production [20,32,36]. Yet, concerns remain about iPSC-derived hepatocytes to resemble adult hepatocytes and several reports suggest a fetal phenotype instead [37,38]. In an attempt to improve maturation and differentiation efficiency, several protocols and culture settings have been proposed but there is yet no consensus on a standardized approach to generate functional,

mature hepatocytes [39]. In this study, we used a commercially available iPSC-derived hepatocyte model which was capable of net glucose production, although considerably less than primary hepatocytes. This could indeed be due to a fetal phenotype that reflects in a decreased capacity for net glucose production. Indeed, gluconeogenesis is known to be absent in the fetal liver but it increases rapidly in the liver of newborns [40]. Although in our experimental model glucose production probably arises from a combination of glycogenolysis and gluconeogenesis, the reduced net output could be attributed to decreased gluconeogenesis compared to primary hepatocytes due to an immature phenotype of the cells.

Upcyte hepatocytes were initially generated to overcome the limitations of primary hepatocytes by inducing their proliferation and re-differentiation showing many basic hepatocyte markers and functionality [21,22,41]. Initial comparison to HepG2 cells revealed an increase expression of gluconeogenesis-related genes *G6PC* and *PEPCK* and the authors hypothesized that these cells would be better capable of gluconeogenesis and glycogen synthesis [41]. A recent study showed that upcyte hepatocytes display similarities with HepG2 in terms of energy metabolism including increased glucose uptake, lactate secretion, reduced glycogen levels and signaling pathway activation associated with hepatocellular carcinoma [23]. This is in line with our observations that although upcyte hepatocytes were capable of glucose net production, this was at levels similar to HepG2 cells.

Hepatic organoids emerged as an exciting possibility to generate patient-derived expandable hepatocytes and recent progress started to determine their exact application landscape to study liver metabolism and disease [24,25]. In this work, we used epithelial organoids established from adult intrahepatic cholangiocytes. These bipotent cells possess a primarily cholangiocyte phenotype but retain the potential to, at least partially, transdifferentiate towards hepatocyte-like cells [25]. Recently a study showed that under optimized culture conditions, adult-derived liver organoid expression levels of *G6PC* and *PCK1* are similar to primary hepatocytes. The same study showed the possibility to perform a glucose production assay in Matrigel-embedded HepG2 clusters [42]. However, no clear protocol has been established for these measurements, as scaffold-embedded organoids cultures present several challenges compared to cells grown as monolayers. The repeated washing of the cells prior to glucose production initiation is imperative, as any residual glucose present from the previous culture phase might lead to an overestimation of glucose released by the cells. This is especially challenging when culture wells contain Matrigel domes, which could potentially release glucose traces also after repeated

washing steps. Furthermore, normalization can be difficult. For this study we opted to normalize metabolic readouts with total protein amount which is clearly challenging when the cells are cultured in biological, protein-rich scaffold such as Matrigel. Determining the total amount of cells also revealed to be challenging for organoids, as these cells grow in compact, three-dimensional structures and an accurate estimation of the total amount of cells remains difficult. Total DNA normalization has been proposed as a valid alternative for metabolomics studies [43]. Despite this, considering the high degree of aneuploidy in HepG2 cells [44], as well as the known polyploidy generally observed in hepatocytes [45], we questioned the utility of this approach for this study. For these reasons, we decided to extract the organoids from the scaffold prior to the 12 h incubation, which was conducted in Eppendorf tubes after repeated washing, from which we could lyse the cells and measure the total protein amount. Despite these challenges, we were capable of measuring net glucose production from liver organoids which was notably higher than all hepatocyte models, with the exception of primary hepatocytes. Yet, concerns about glucose and Matrigel traces during the incubation period remain, and further research needs to be conducted to establish robust glucose production assays in scaffold-embedded organoids.

Glucose production is a highly regulated process, as hepatocytes quickly respond to hormonal stimulation, substrate availability and intracellular molecular changes to maintain glucose homeostasis [2,5,8]. We observed clear induction of gluconeogenic genes *G6PC* and *PCK1* after incubation in GP medium compared to Fed medium, in which glucose was abundant and in the presence of insulin. This was noticeable in all hepatocyte models, with primary hepatocytes increasing the expression of both genes approximately 100-fold. This trend was not observed for the expression of *FBP1*, which was upregulated only 2-fold in primary hepatocytes and upcyte hepatocytes, while we observed a downregulation in organoids and HepG2 cells. This can be explained by the fact that FBPase has been shown to be mainly regulated allosterically, rather than at the transcription level, such as by AMP mediated inhibition [46].

Glucose and lipid metabolism are connected in a multitude of ways and disturbances of glucose metabolism can in turn lead to pathological changes in lipids. Examples include dyslipidemia often found in patients with diabetes [47] or fatty liver disease caused by glycogen storage diseases [48]. In turn, disorders of lipid metabolism are often associated with dysregulation in glucose metabolism [49]. Comparing the total lipidome of different hepatocyte models is challenging due to profound differences in the starting material, donor-to-donor variations,

growing and differentiation medium composition and subsequent substrate availability that can greatly alter the lipid composition. Furthermore, biological differences in metabolic pathways can result in drastic differences. It has been shown, for example, that de-differentiation of primary hepatocytes as a result of *in vitro* culture results in marked increase in SFA and MUFA with a decrease in PUFA over time [50]. Overall, we observed a similar trend in glycerolipids when comparing primary hepatocytes to the other hepatocyte models possibly indicating that they possess a de-differentiated phenotype. When comparing individual lipid species, it has been shown that iPSC-derived hepatocytes possess a closer lipid profile to primary hepatocytes compared to HepG2 [32]. In our study, we observed closest similarity with organoids, a model that was not tested in that study. We note however that comparing the total lipid profile in terms of concentration poses challenges. This is because of the uneven abundance of the different classes, where the highest abundant ones, primarily triglycerides, are largely responsible for the most pronounced differences between the models. In our multivariate analysis, we attributed the same weight to each class and lipid species. Different multivariate techniques could potentially elucidate other associations between different models.

The most direct link between lipid and glucose metabolism is reflected in the hepatic synthesis or breakdown of fatty acids, stored as triglycerides, as a response of nutrient availability. Fatty acid beta-oxidation is a key process to release the energy needed for the production of glucose during gluconeogenesis [7]. Alternatively, *de novo* lipogenesis converts excess carbohydrates into fatty acids, later incorporated into triglycerides [51]. Overall, our experimental glucose production condition seems to induce a downregulation of several TG species in primary hepatocytes and organoids. This could be attributed to an activated beta-oxidation pathway which could in turn explain the increase in net glucose production compared to iPSC-Hep and HepG2 in which TG content was minimally altered. In this study we did not directly assess beta-oxidation, and further studies and direct assays are needed to provide a functional proof. In contrast to primary hepatocytes and organoids, Upcyte-Hep significantly increased several TG species under the same conditions. We hypothesize that our glucose production condition, which contained no glucose but abundant amounts of lactate and pyruvate could lead to a great availability of acetyl-CoA, a major lipogenic precursor. Decreased gluconeogenic flux and energy demand could therefore lead Upcyte-Hep to utilize acetyl-CoA for *de novo* lipogenesis, rather than breakdown via the Krebs pathway. It is possible, therefore, that decreased glucose production rates in iPSC-Hep, HepG2 and Upcyte-Hep correlate with decreased fatty acid beta-oxidation. Indeed it has been reported that HepG2 possess a significantly lesser basal oxidation

rate compared to primary hepatocytes rates [17]. Overall, our data suggest that this experimental approach does not seem to induce TG breakdown in iPSC-Hep, HepG2 and Upcyte-Hep. Further studies are needed to identify experimental conditions that are compatible with these hepatocyte models to induce fatty acid beta-oxidation in combination with glucose production. This could include a pre-starvation period to deplete stored glycogen reserves or a period of fatty acid treatments to increase the TG content in the cells prior to the glucose production challenge.

Triglycerides are stored inside of lipid droplets in the cytoplasm of the cells that act as dynamic organelles, alternating between periods of growth and consumption [52]. Triglycerides are also secreted by hepatocytes in very low-density lipoproteins (VLDL) in a highly regulated process to meet energetic demands of extrahepatic tissues. Indeed, glucagon has been reported to decrease VLDL release in hepatocytes [53]. It has been observed that changes in cell membrane composition, as a result of dietary or environmental factors, can alter cell permeability and receptor stability that can contribute to pathologies such as insulin resistance and other metabolic disorders. Cell membrane components, such as phospholipid and sphingolipids are an integral part of lipid droplets and VLDL and their synthesis, breakdown or release is interlinked with the metabolic processes to maintain energy homeostasis in the organism. The two most abundant phospholipids, PC and PE were highly abundant in all hepatocyte models compared to other lipid classes, with the exception of TGs. Glucose production conditions significantly decreased several PE species in primary hepatocytes and, to a lesser extent, in HepG2 cells while PC species did not show any significant change. A change in PE could partially be explained by an alteration in VLDL synthesis and release, or structural changes of lipid droplets that would result in an alteration of the synthesis and breakdown of membrane components. Organoids showed significantly decreased PE and PC species in the glucose production condition while an increase was observed in iPSC-Hep and Upcyte-Hep.

Overall, a great diversity of response was observed across all lipid classes, indicating profound differences between the hepatocyte models. Further studies and fundamental research is needed to identify the links between lipid metabolism in conjunction with energy homeostasis. Our data seem to suggest a closer relationship in lipid composition and changes between primary hepatocytes and organoids compared to iPSC-Hep, Upcyte-Hep and HepG2. This was ultimately also reflected in the glucose production rates.

5. Conclusion

With this study, we aimed at further advancing the scientific community's pursuit of establishing and characterizing an accurate and dependable cellular tool that can substitute primary hepatocytes for *in vitro* studies. Hepatocytes are responsible for a plethora of functions and a complete cellular model with *in vivo*-like accuracy has yet to be developed. Hence, researchers are trying to identify and categorize different hepatocyte models for their suitability on specific applications. Here, we focused on energy metabolism, comparing several hepatocyte models to primary hepatocytes on glucose production, gluconeogenic gene regulation and lipid content. This study suggests that for glucose production studies, liver organoids might possess the highest net production capacity after primary hepatocytes. Other models also show net production but at lower levels. In terms of gene regulation, we observed induction of key gluconeogenic genes in all models, suggesting that, although net glucose production might drastically differ, all models could be useful to study gluconeogenesis gene regulation. Finally, lipidomics analysis revealed promising similarity between primary hepatocytes and liver organoids compared to other models. However, further studies need to be conducted to confirm organoid models as representative of fully mature, differentiated and metabolically competent hepatocytes.

6. Limitations of this study

In this section, we would like to explicitly address the limitations of this study. The first notable limitation is the use of cells derived from a single donor which may limit the extrapolation of some of the conclusions to a broader population. Donor-to-donor variation is an important variable that can drastically influence cell metabolism. Furthermore, the differentiation process of organoids and iPSC-derived hepatocytes can vary between donors and experiment. A bigger donor cohort of all hepatocyte models (with exception of HepG2 as it represents a single donor line) should be included in future studies. Gene expression analysis revealed high degree of regulation, yet this was not confirmed at the protein level. Subsequent protein expression profile should be addressed in future studies. Similarly, hepatocyte phenotype characterization was performed on gene expression. Yet, although indicative of the cell's phenotype, functional proof is not included in this work and should be addressed in follow-up characterization.

Author contributions

Flavio Bonanini and Madhulika Singh contributed equally to this manuscript. Flavio Bonanini: Conceptualization, Data curation, Formal analysis, Investigation, Methodology, Visualization,

Writing – original draft, Writing – review and editing. Madhulika Singh: Conceptualization, Data curation, Formal analysis, Investigation, Methodology, Visualization, Writing – original draft, Writing – review and editing. Hong Yang: Formal analysis, Data curation. Dorota Kurek: Funding acquisition, Project administration, Supervision, Writing – review and editing. Amy Harms: Funding acquisition, Project administration, Supervision, Writing – review and editing. Adil Mardinoglu: Funding acquisition, Project administration, Supervision. Thomas Hankemeier: Funding acquisition, Project administration, Writing – review and editing.

Declaration of competing interests

Flavio Bonanini and Dorota Kurek are employees of Mimetas BV, which markets advanced *in vitro* system for drug development. The authors declare they have no additional conflict of interests.

Acknowledgements

This project has received funding from the European Union's Horizon 2020 research and innovation program under the Marie Skłodowska-Curie grant agreement No 812616.

We would like to acknowledge Vincent Vermeulen for helping in the maintenance of liver organoids.

References

[1] Sharabi K, Tavares CDJ, Rines AK, Puigserver P. Molecular pathophysiology of hepatic glucose production. Vol. 46, Molecular Aspects of Medicine. Elsevier Ltd; 2015. p. 21–33.

[2] Nordlie RC, Foster JD, Lange AJ. Regulation of glucose production by the liver. Annu Rev Nutr. 1999;19:379–406.

[3] Koutsifeli P, Varma U, Daniels LJ, Annandale M, Li X, Neale JPH, et al. Glycogen-autophagy: Molecular machinery and cellular mechanisms of glycophagy. Vol. 298, Journal of Biological Chemistry. American Society for Biochemistry and Molecular Biology Inc.; 2022.

[4] Adeva-Andany MM, González-Lucán M, Donapetry-García C, Fernández-Fernández C, Ameneiros-Rodríguez E. Glycogen metabolism in humans. Vol. 5, BBA Clinical. Elsevier B.V.; 2016. p. 85–100.

[5] Zhang X, Yang S, Chen J, Su Z. Unraveling the regulation of hepatic gluconeogenesis. Vol. 10, Frontiers in Endocrinology. Frontiers Media S.A.; 2019.

[6] Chen L, Chen XW, Huang X, Song BL, Wang Y, Wang Y. Regulation of glucose and lipid metabolism in health and disease. Vol. 62, Science China Life Sciences. Science in China Press; 2019. p. 1420–58.

[7] Rui L. Energy metabolism in the liver. Compr Physiol. 2014;4(1):177–97.

[8] Petersen MC, Vatner DF, Shulman GI. Regulation of hepatic glucose metabolism in health and disease. Vol. 13, Nature Reviews Endocrinology. Nature Publishing Group; 2017. p. 572–87.

[9] Weinstein DA, Steuerwald U, De Souza CFM, Derks TGJ. Inborn Errors of Metabolism with Hypoglycemia: Glycogen Storage Diseases and Inherited Disorders of Gluconeogenesis. Vol. 65, Pediatric Clinics of North America. W.B. Saunders; 2018. p. 247–65.

[10] Jiang S, Young JL, Wang K, Qian Y, Cai L. Diabetic-induced alterations in hepatic glucose and lipid metabolism: The role of type 1 and type 2 diabetes mellitus (Review). Vol. 22, Molecular Medicine Reports. Spandidos Publications; 2020. p. 603–11.

[11] Gastaldelli A, Baldi S, Pettiti M, Toschi E, Camastra S, Natali A, et al. Influence of Obesity and Type 2 Diabetes on Gluconeogenesis and Glucose Output in Humans A Quantitative Study [Internet]. Vol. 49, DIABETES. 2000. Available from: http://diabetesjournals.org/diabetes/article-

pdf/49/8/1367/365058/10923639.pdf
[12] Roh E, Song DK, Kim MS. Emerging role of the brain in the homeostatic regulation of energy and glucose metabolism. Vol. 48, Experimental and Molecular Medicine. Nature Publishing Group; 2016.
[13] Van Den Berghe G. Disorders of gluconeogenesis. Vol. 19, J. Inher. Metab. Dis. 1996.
[14] Özen H, Bayraktar Y. Glycogen storage diseases: New perspectives Professor, Series Editor. World J Gastroenterol [Internet]. 2007;13(18):2541–53. Available from: www.wjgnet.comhttp://www.wjgnet.com/1007-9327/13/2541.asp
[15] Lee CH, Olson P, Evans RM. Minireview: Lipid metabolism, metabolic diseases, and peroxisome proliferator-activated receptors. In: Endocrinology. 2003. p. 2201–7.
[16] Zou H, Liu Q, Meng L, Zhou J, Da C, Wu X, et al. Chemical genetic-based phenotypic screen reveals novel regulators of gluconeogenesis in human primary hepatocytes. NPJ Genom Med. 2018 Dec 1;3(1).
[17] Nagarajan SR, Paul-Heng M, Krycer JR, Fazakerley DJ, Sharland AF, Andrew X, et al. Lipid and glucose metabolism in hepatocyte cell lines and primary mouse hepatocytes: a comprehensive resource for in vitro studies of hepatic metabolism. Am J Physiol Endocrinol Metab [Internet]. 2019;316:578–89. Available from: http://www.ajpendo.org
[18] Kalemba KM, Wang Y, Xu H, Chiles E, McMillin SM, Kwon H, et al. Glycerol induces G6pc in primary mouse hepatocytes and is the preferred substrate for gluconeogenesis both in vitro and in vivo. Journal of Biological Chemistry. 2019 Nov 29;294(48):18017–28.
[19] Matsumoto M, Sakai M. Glucose Production Assay in Primary Mouse Hepatocytes [Internet]. Vol. 2, Iss. 2012. Available from: http://www.bio-protocol.org/e284
[20] Mitani S, Takayama K, Nagamoto Y, Imagawa K, Sakurai F, Tachibana M, et al. Human ESC/iPSC-Derived Hepatocyte-like Cells Achieve Zone-Specific Hepatic Properties by Modulation of WNT Signaling. Molecular Therapy. 2017 Jun 7;25(6):1420–33.
[21] Tolosa L, Gómez-Lechón MJ, López S, Guzmán C, Castell J V., Donato MT, et al. Human upcyte hepatocytes: Characterization of the hepatic phenotype and evaluation for acute and long-term hepatotoxicity routine testing. Toxicological Sciences. 2016 Jul 1;152(1):214–29.
[22] Levy G, Bomze D, Heinz S, Ramachandran SD, Noerenberg A, Cohen M, et al. Long-term culture and expansion of primary human hepatocytes. Nat Biotechnol. 2015 Dec 1;33(12):1264–71.
[23] Scheffschick A, Babel J, Sperling S, Nerusch J, Herzog N, Seehofer D, et al. Primary-like Human Hepatocytes Genetically Engineered to Obtain Proliferation Competence as a Capable Application for Energy Metabolism Experiments in In Vitro Oncologic Liver Models. Biology (Basel). 2022 Aug 1;11(8).
[24] Lehmann V, Schene IF, Ardisasmita AI, Liv N, Veenendaal T, Klumperman J, et al. The potential and limitations of intrahepatic cholangiocyte organoids to study inborn errors of metabolism. J Inherit Metab Dis. 2022 Mar 1;45(2):353–65.
[25] Huch M, Gehart H, Van Boxtel R, Hamer K, Blokzijl F, Verstegen MMA, et al. Long-term culture of genome-stable bipotent stem cells from adult human liver. Cell. 2015 Jan 15;160(1–2):299–312.
[26] Broutier L, Andersson-Rolf A, Hindley CJ, Boj SF, Clevers H, Koo BK, et al. Culture and establishment of self-renewing human and mouse adult liver and pancreas 3D organoids and their genetic manipulation. Nat Protoc. 2016;11(9):1724–43.
[27] Matyash V, Liebisch G, Kurzchalia T V., Shevchenko A, Schwudke D. Lipid extraction by methyl-terf-butyl ether for high-throughput lipidomics. J Lipid Res. 2008;49(5):1137–46.
[28] Zhang Z, Singh M, Kindt A, Wegrzyn AB, Pearson MackenzieJ, Ali A, et al. Development of a targeted hydrophilic interaction liquid chromatography-tandem mass spectrometry based lipidomics platform applied to a coronavirus disease severity study. J Chromatogr A [Internet]. 2023;464342. https://www.sciencedirect.com/science/article/pii/S0021967323005678
[29] Sefried S, Häring HU, Weigert C, Eckstein SS. Suitability of hepatocyte cell lines HepG2, AML12 and THLE-2 for investigation of insulin signalling and hepatokine gene expression. Open Biol. 2018 Oct 1;8(10).
[30] Yu S, Meng S, Xiang M, Ma H. Phosphoenolpyruvate carboxykinase in cell metabolism: Roles and mechanisms beyond gluconeogenesis. Vol. 53, Molecular Metabolism. Elsevier GmbH; 2021.
[31] Hartler J, Köfeler HC, Trötzmüller M, Thallinger GG, Spener F. Assessment of lipidomic species in hepatocyte lipid droplets from stressed mouse models. Sci Data. 2014 Dec 23;1.
[32] Kiamehr M, Alexanova A, Viiri LE, Heiskanen L, Vihervaara T, Kauhanen D, et al. hiPSC-derived hepatocytes closely mimic the lipid profile of primary hepatocytes: A future personalised cell model for studying the lipid metabolism of the liver. J Cell Physiol. 2019 Apr 1;234(4):3744–61.
[33] Huggett ZJ, Smith A, De Vivo N, Gomez D, Jethwa P, Brameld JM, et al. A Comparison of Primary Human Hepatocytes and Hepatoma Cell Lines to Model the Effects of Fatty Acids, Fructose and Glucose on Liver Cell Lipid Accumulation. Nutrients. 2023 Jan 1;15(1).
[34] Xu H, Wang Y, Kwon H, Shah A, Kalemba K, Su X, et al. Glucagon changes substrate preference in gluconeogenesis. Journal of Biological Chemistry. 2022 Dec 1;298(12).

[35] Molinaro A, Becattini B, Solinas G. Insulin signaling and glucose metabolism in different hepatoma cell lines deviate from hepatocyte physiology toward a convergent aberrant phenotype. Sci Rep. 2020 Dec 1;10(1).
[36] Holmgren G, Ulfenborg B, Asplund A, Toet K, Andersson CX, Hammarstedt A, et al. Characterization of human induced pluripotent stem cell-derived hepatocytes with mature features and potential for modeling metabolic diseases. Int J Mol Sci. 2020 Jan 2;21(2).
[37] Kvist AJ, Kanebratt KP, Walentinsson A, Palmgren H, O'Hara M, Björkbom A, et al. Critical differences in drug metabolic properties of human hepatic cellular models, including primary human hepatocytes, stem cell derived hepatocytes, and hepatoma cell lines. Biochem Pharmacol. 2018 Sep 1;155:124–40.
[38] Raju R, Chau D, Notelaers T, Myers CL, Verfaillie CM, Hu WS. In vitro pluripotent stem cell differentiation to hepatocyte ceases further maturation at an equivalent stage of e15 in mouse embryonic liver development. Stem Cells Dev. 2018 Jul 1;27(13):910–21.
[39] Graffmann N, Scherer B, Adjaye J. In vitro differentiation of pluripotent stem cells into hepatocyte like cells – Basic principles and current progress. Vol. 61, Stem Cell Research. Elsevier B.V.; 2022.
[40] Girard J. Glueoneogenesis in Late Fetal and Early Neonatal Life [Internet]. Vol. 50, Biol. Neonate. 1986. Available from: http://karger.com/neo/article-pdf/50/5/237/2273521/000242605.pdf
[41] Tolosa L, Gómez-Lechón MJ, López S, Guzmán C, Castell J V., Donato MT, et al. Human upcyte hepatocytes: Characterization of the hepatic phenotype and evaluation for acute and long-term hepatotoxicity routine testing. Toxicological Sciences. 2016 Jul 1;152(1):214–29.
[42] Gamboa CM, Wang Y, Xu H, Kalemba K, Wondisford FE, Sabaawy HE. Optimized 3d culture of hepatic cells for liver organoid metabolic assays. Cells. 2021 Dec 1;10(12).
[43] Silva LP, Lorenzi PL, Purwaha P, Yong V, Hawke DH, Weinstein JN. Measurement of DNA concentration as a normalization strategy for metabolomic data from adherent cell lines. Anal Chem. 2013 Oct 15;85(20):9536–42.
[44] Zhou B, Ho SS, Greer SU, Spies N, Bell JM, Zhang X, et al. Haplotype-resolved and integrated genome analysis of the cancer cell line HepG2. Nucleic Acids Res. 2019 May 7;47(8):3846–61.
[45] Wang MJ, Chen F, Lau JTY, Hu YP. Hepatocyte polyploidization and its association with pathophysiological processes. Vol. 8, Cell Death and Disease. Springer Nature; 2017.
[46] Liu GM, Zhang YM. Targeting FBPase is an emerging novel approach for cancer therapy. Vol. 18, Cancer Cell International. BioMed Central Ltd.; 2018.
[47] Sargsyan A, Herman MA. Regulation of Glucose Production in the Pathogenesis of Type 2 Diabetes. Vol. 19, Current Diabetes Reports. Current Medicine Group LLC 1; 2019.
[48] Leuzinger Dias C, Maio I, Brandão JR, Tomás E, Martins E, Santos Silva E. Fatty Liver Caused by Glycogen Storage Disease Type IX: A Small Series of Cases in Children. GE Port J Gastroenterol. 2019 Oct 1;26(6):430–7.
[49] Wanders RJA, Visser G, Ferdinandusse S, Vaz FM, Houtkooper RH. Mitochondrial fatty acid oxidation disorders: Laboratory diagnosis, pathogenesis, and the complicated route to treatment. Vol. 9, Journal of Lipid and Atherosclerosis. Korean Society of Lipid and Atherosclerosis; 2020. p. 313–33.
[50] Kiamehr M, Heiskanen L, Laufer T, Düsterloh A, Kahraman M, Käkelä R, et al. Dedifferentiation of primary hepatocytes is accompanied with reorganization of lipid metabolism indicated by altered molecular lipid and miRNA profiles. Int J Mol Sci. 2019 Jun 2;20(12).
[51] Ameer F, Scandiuzzi L, Hasnain S, Kalbacher H, Zaidi N. De novo lipogenesis in health and disease. Vol. 63, Metabolism: Clinical and Experimental. W.B. Saunders; 2014. p. 895–902.
[52] Olzmann JA, Carvalho P. Dynamics and functions of lipid droplets. Vol. 20, Nature Reviews Molecular Cell Biology. Nature Publishing Group; 2019. p. 137–55.
[53] Guettet ' C, Mathe D, Riottot ' M, Lutton ' C. Effects of chronic glucagon administration on cholesterol and bile acid metabolism. Vol. 963, Biochimica et Biophyka Acta. 1988.

Supplementary Material

Table S1. Concentration of internal standard mix spiked in liver cell matrices.

Internal standards mix	Concentration (nmol mL^{-1})
PC 15:0/18:1-d7	17.00
PE 15:0/18:1-d7	0.56
PS 15:0/18:1-d7	0.51
PG 15:0/18:1-d7	3.14
PI 15:0/18:1-d7	0.94
LPC 18:1-d7	3.78
LPE 18:1-d7	0.82
CE 18:1-d7	42.54
DG 15:0/18:1-d7	1.36
TG 15:0/18:1-d7/15:0	5.42
SM 18:1;O2/18:1-d9	3.25
LPG 17:1	0.16
LPI 17:1	0.31
LPS 17:1	0.22
Cer 18:1;O2/16:0-d9	1.83
Cer 18:0;O2/16:0-d9	0.73
Hex-Cer 18:1;O2/16:0-d9	0.38
Lac-Cer d18:1;O2/16:0-d9	1.03

Table S2. In supplementary excel.

Sheet 1. Lipid targets in HILIC-MS/MS acquisition method. The internal standards are highlighted in yellow.
Sheet 2. Lipid concentration expressed in µM per mg of protein.
Sheet 3. Statistical significance (p-value) of endogenous lipid species in four matrices with PHH as reference.
Sheet 4. Lipid species that have been altered significantly ($FC \geq 1.5$ or $FC \leq 0.7$, p-value < 0.05) in the GP medium.